



Synthesis, Crystal structure, DFT calculations and Antimicrobial activity of 4-(4-Fluoro-phenyl)-2,6-dimethyl-1,4-dihydro-pyridine-3,5-dicarboxylic acid diethyl ester



D. Parthasarathi,^a M. Syed Ali Padusha,^{a*} S. Suganya,^b P. Kumaradhas,^{b*} Fares M Howari,^c

Yousef Nazzal,^c Cijo Madathil Xavier,^c A. Meera Moydeen,^d Ayyiliath M. Sajith^e

^aPost Graduate and Research Department of Chemistry, Jamal Mohamed College, Bharathidasan University, Tiruchirappalli, Tamilnadu, 620 020, India

^bLaboratory of X-Ray Crystallography and Computational Molecular biology, Department of Physics, Periyar University, Salem-636 01, India

^cCollege of Natural and Health Sciences, Zayed University, Abudhabi, P.O. 144534, United Arab Emirates

^dDepartment of Chemistry, College of Science, King Saud University, Riyadh 11451, Saudi Arabia

^eOrtin laboratories Pvt.Ltd, Malkapur Village, Choutuppal Mandal, Hyderabad, Telengana-508252, India

Abstract

The title compound was synthesized and confirmed by FT-IR, ¹H, ¹³C NMR analysis. The molecular structure of the compound was precisely determined by Single Crystal X-ray Diffraction (SC-XRD) analysis. The crystallized compound shows P21/C & monoclinic crystal system with cell parameters a = 9.7768 (5), b = 7.4005(3) and c = 24.8099 (12), β=93.734(2)°. The structural and electronic properties of the compound were carried out by Density Functional Theory (DFT) calculations. The compound exhibited H-bonding between N1-H1A----O1 with bond distance 2.98(7) Å. The energy gap Egap 4.53eV and Egap= 4.34eV for crystal and DFT method respectively. The molecular orbitals energies were studied through Highest Unoccupied Molecular Orbital (HOMO) and Lowest Unoccupied Molecular Orbital (LUMO) analysis. The softness and hardness of the molecule was studied through Global Chemical Reactivity Descriptors (GCRD). The electrophilic and nucleophilic characters were studied through Molecular Electrostatic Potential (MEP) studies. The antimicrobial studies were carried out by *in-vitro* method against 6 microorganisms. © 2020 NIODC. All rights reserved

Keywords: 1,4 Dihydro pyridine; Ethyl acetoacetate; Crystal structure; MEP; DFT calculations

1. Introduction

Diversely substituted 1,4 dihydropyridine (1,4 DHP) scaffolds have gained significant attention in the field of heterocyclic chemistry. The first report on the synthesis of 1,4 DHP derivatives was reported by Arthur Hantzsch in 1881[1]. The wide range of pharmacological properties like antihypertensive, anti-anginal and calcium channel blockers displayed by these classes of analogues highlights the versatility of this heterocyclic framework. Especially 1,4 DHP derivatives were extensively used for the treatment of hypertension and cardiovascular diseases [2,4]. Some important drug molecules are available in

the market such as Nefidipine, Felodipine, Amlodipine, Nivaldipine, Isradipine and Nimodipine have 1,4 DHP core unit in their structure [5-11]. The first-generation calcium channel blocker Nefidipine was first reported by Bayer and subsequent development of 2nd and 3rd generation novel chemical entities based on this core for their use as calcium antagonist and antihypertensive agents emphasize its medicinal relevance [12,-14]. The presence of this vital 1,4 DHP core in the calcium channel blocker drug prompted us to further investigate the possible structural modifications in

*Corresponding author e-mail: sp@jmc.edu; (Dr. M. SYED ALI PADUSHA).

Receive Date: 27 April 2021, Revise Date: 20 May 2021, Accept Date: 20 June 2021

DOI: 10.21608/EJCHEM.2021.74007.3667

©2021 National Information and Documentation Center (NIDOC)

1,4 DHP binding site [15]. The pharmacological activity is mainly due to the presence of aromatic group at C4 and esters and acyl/acetyl groups at C3 and C5 positions respectively [16-18]. Among them most of the 1,4 DHP possess esters and acetyl groups at C3 and C5 positions. Only a limited number of reports are available on the unsymmetrical 1,4 DHP analogues having acetyl group at C3 and C5 positions [19]. Structure Activity Relationship (SAR) studies reveals that the presence of substituents at C4 position makes them as tissue selectivity and calcium channel modulators [20,21]. Apart from the use of cardiovascular activities, 1,4 dihydropyridine derivatives possess good antimicrobial properties [22,23].

Studies by various researchers on the biological aspects of this medicinally relevant core demand the development of novel methodologies that allow diversity around this framework. Among the several synthetic protocols employed, one pot multicomponent reaction (MCR) still remains a versatile tool for the synthesis of 1,4 DHP. Conversely, these MCRs have some disadvantages such as the requirement of high temperature, expensive catalyst, tedious work procedures, and long reaction time [24-26].

The biochemical utility of 1,4 DHP heterocyclic core part encourages in developing the environmentally benign synthetic methods, achieved through multicomponent protocol. Present work investigates the synthesis of 4-(4-Fluoro-phenyl)-2,6-dimethyl-1,4-dihydro-pyridine-3,5-dicarboxylic acid diethyl ester. The synthesized compound was confirmed by FT-IR, ^1H , ^{13}C NMR analysis. The molecular structure of the compound was precisely determined by SC-XRD analysis. The geometrical parameters of the crystal are compared with DFT parameters.

2. Materials and Methods

Ethyl acetoacetate and 4-fluoro benzaldehyde were purchased from sigma Aldrich. Ammonium acetate was purchased from Merck. All chemicals were used without purging. Thin Layer chromatography was performed using silica gel (Mesh120) with glass plates. Melting point of the compound was determined using the Buchi apparatus. The FT-IR spectrum was recorded on Perkin Elmer spectrophotometer using KBr pellets. ^1H -NMR and ^{13}C -NMR spectra were recorded on Bruker high-

performance Fourier Transform- Nuclear Magnetic Resonance spectrometer (FT-NMR-400 MHz). The chemical shift (δ) and coupling constants (J) were measured by ppm and Hz respectively.

2.1. Synthetic procedure of 1,4 DHP

A mixture of 4-fluoro benzaldehyde (0.01M), ethyl acetoacetate (0.02 M) and ammonium acetate (0.015 M) were dissolved in 30 mL ethanol+water and transferred into 100 mL round bottom flask. The reaction mixture was stirred for 2 h at room temperature. The completion of the reaction was ensured by TLC. After completion of the reaction, a solid mass precipitated out that was filtered off, washed with distilled water and dried in vacuum. The crude solid was recrystallized using pure ethanol and developed crystal is shown in **Fig.1**.



Fig. 1. Grown crystal

Yellow color Solid; yield-90%; m.p. 256-258 oC; FT-IR: 3343 cm^{-1} (N-H), 2983.54 cm^{-1} (R-CH), 1687.86 ($\text{C}=\text{O}$), 1489.37 ($\text{C}=\text{C}$), 1211.90 (C-F); ^1H NMR (400 MHz, CDCl_3) δ 7.32 – 7.28 (m, 2H, Ar-H), 7.14 (d, $J = 8.1$ Hz, 2H, Ar-H), 5.93 (s, 1H, -NH), 4.94 (s, 1H, -CH), 4.17 – 4.00 (m, 4H, -CH₂), 2.34 – 2.28 (m, 6H, -OCH₃), 1.22 (t, $J = 7.1$ Hz, 6H-CH₃). ^{13}C NMR (101 MHz, CDCl_3) δ 167.43(-C=O), 146.89, 146.84, 144.03, 131.35, 130.90, 129.84, 119.88, 103.81, 103.60, 59.86, 39.53, 39.33, 19.69, 19.43, 14.28.

2.2. X-Ray structure analysis and refinement

The crystallographic intensity data of the compound were collected at room temperature (293 K) on a Bruker D8 Quest Eco diffractometer using $\text{MoK}\alpha$ radiation (0.71073 Å) and the APEX-III program was used to monitor the data collection [27]. The Bruker SAINT Software package was used for cell refinement and data reduction. The absorption effect data were corrected using the multi scan

method (SADABS) [28]. The softwares such as SHELXS-2014 & SHELXL-2014 were used to refine the crystal structure of the compound [29,30]. A total of 46007 reflections were observed from the monoclinic crystal system. The non-hydrogen atoms were resolved anisotropically and hydrogen atoms were refined geometrically [C-H = 0.96 Å] using riding model $U_{iso}(H) = 1.5 U_{eq}(C)$. $U_{iso} = 1.5$ (Cmethyl). The crystal packing and geometrical parameters were accomplished via MERCURY and ORTEP [31,32].

2.3. Computational details

The quantum chemical calculations were computed by DFT- Gaussian 09 version by B3LYP/6-311++G(d,p) method. The Gauss view 5.0 program was used to interpret the data and structural visualization of the compound [33]. The geometrical structure, HOMO-LUMO, MEP, MPA, and NPA of the compound were acquired through DFT analysis [34].

2.4. Antimicrobial activity

The microorganisms were obtained from National Chemical Lab (NCL) Pune. The antimicrobial activity of the title compound was analyzed by well diffusion method against two gram positive (*Bacillus subtilis* & *Staphylococcus aureus*), two gram negative bacteria (*Escherichia coli* & *Pseudomonas*) and two fungi (*Candida albicans* & *Aspergillus niger*) at 100 µL. The effect produced by the sample was compared with control (standard amoxicillin 100µL disc for bacteria; Nystatin 100µL disc for fungi) and solvent-DMSO.

3. Results and Discussions

3.1. FT-IR stretching frequencies

The IR spectrum of the compound is shown in **Fig. S1**. The N-H peak appeared at 3343 cm^{-1} . The existence of a band at 2983 cm^{-1} is corresponding to aliphatic C-H stretching. A peak observed at 1489 cm^{-1} is assigned to C=C stretching. A peak appeared at 1687 cm^{-1} is corresponding to C=O group. A peak observed at 1211 cm^{-1} is due to the presence of C-F stretching [35,36]

3.2. ^1H and ^{13}C NMR analysis

The ^1H NMR spectrum of the compound was recorded using CDCl_3 solvent and its spectrum is

shown in **Fig. S2**. The aromatic protons are observed in the region δ 7.32-7.14 ppm. A singlet observed at δ 4.94 ppm is attributed to -CH proton. A multiplet observed from δ 4.17 to 4.00 ppm is corresponding to CH_2 protons. The existence of a peak at δ 5.93 ppm is attributed to NH proton. The presence of methyl group in the pyridine ring is observed by a singlet observed at δ 2.32 ppm. A triplet observed in the region δ 1.23-1.20 ppm is assigned to CH_3 proton.

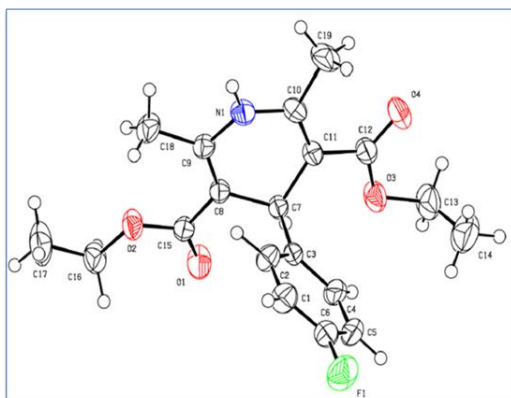
The ^{13}C NMR spectrum of the compound is shown in **Fig. S3**. A signal appeared at δ 167.43 ppm confirms the presence of C=O. A multiplet appeared in the region δ 144.76 -139.06 ppm is assigned to aromatic carbon. A signal observed at δ 39.33 ppm is corresponding to benzylidene CH carbon. The presence of methyl carbon at pyridine ring is ensured by the appearance of a peak at δ 19.49 ppm. A peak appeared at δ 14.28 ppm is attributed to methylene of ethoxy carbon and a peak appeared at δ 59.86 ppm is assigned to O- CH_3 carbon [37]

3.3. Single crystal XRD analysis

The crystallized compound ($\text{C}_{19}\text{H}_{22}\text{FNO}_4$) exhibited P21/C monoclinic space group with cell parameters $a = 9.7768$ (5), $b = 7.4005$ (3) and $c = 24.8099$ (12), $\beta = 93.734$ (2)°, $V = 1791.27$ (15) Å³, final R indices [$I > 2\sigma(I)$] = 0.0583 and Goodness of fit on $F^2 = 1.057$. The crystal structure information and refinement data are given in **Table 1** and ORTEP plot of the compound is shown in **Fig. 2**. The dihydro pyridine ring was characterized by flattened boat conformation, N1 and C7 atoms are arranged from the base of the boat plane, which is confirmed by N1C8/C9/C10/C11 atoms. The presence of N—H1A bond is ensured by bond length = 0.84 (2). The bond angle for C10—N1—H1A is 118.8 (16) and C9—N1—H1A is 116.6 (16). Torsion angles are another structural description of the crystallized compound and angles found for C8—C7—C3—C4 = 151.46 (4)° and C11—C7—C3—C4 = -85.73 (16)°. The torsion angles found in the C7—C11—C10—N1 and C7—C8—C9—N1 atoms of pyridine ring are -10.3 (2)° and 8.3 (2)° respectively.

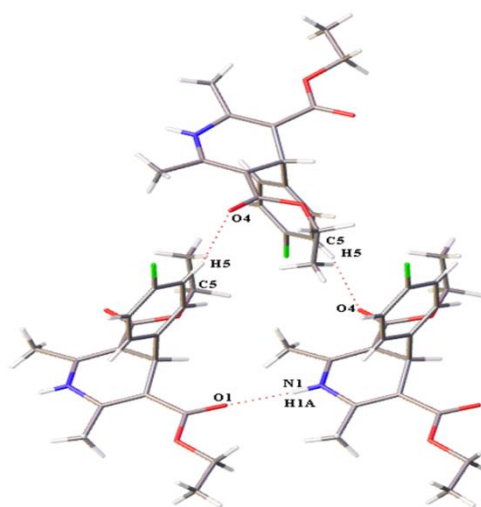
Table 1. Crystallographic information and structure refinement data.

CCDC number	2040803
Molecular formula	C ₁₉ H ₂₂ FNO ₄
Molecular weight	347.37 g/mol
Crystal system & space group	Monoclinic & P2 ₁ /C
Temperature (K)	293
a, b, c (Å)	9.7768(5), 7.4005 (3), 24.8099 (12)
α, β, γ (°)	90, 93.734, 90
V (Å ³)	1791.27 (15)
Z	4
Radiation type	Mo Kα
μ (mm ⁻¹)	0.10
Crystal size (mm)	0.51 x 0.51 x 0.41
Data collection	
Diffractometer	Bruker D8 QUEST ECO
Absorption correction	Multi-scan
T _{min} , T _{max}	0.900, 0.9926
No. of measured, independent at observed [I > 2σ(I)] reflections	46007, 4436, 3757
R _{int}	0.049
Sinθ/λ _{max} (Å ⁻¹)	0.667
Refinement	
R[F ² > 2σ(F ²)], wR (F ²), S	0.058, 0.153, 1.057
No. of reflections	4436
No. parameters	270
H-atom treatment	H atoms treated by a mixture of independent and constrained
Δρ _{max} , Δρ _{min} (eÅ ⁻³)	Refinement 0.28, -0.25

**Fig. 2.** ORTEP plot of the molecule with 50% probability and atom labelling

The torsion angle found for both side of ethoxy groups are C7—O2—C16—C8 = 176.01 (16)° and

C13—O3—C12—C1 = -174.76 (15)° respectively. The selected torsion angles, bond length and bond angles are summarized in **Table S1**. The fractional atomic coordinates and isotropic displacement parameters (Å²) are given in **Table S2**. The flattened boat structure was confirmed from the displacement (Å²) values found for N1 = 0.0158 (15) and C7 = 0.142 (14). The structure of the compound exhibits inter-molecular H-bonding between N1—H1A----O1 with the bond distance of 2.9821(7) Å. The compound also shows intra-molecular H-bonding viz., C—H bonding with neighboring oxygen atom C5—H5...O4 with the bond distance of 3.377(2) Å. H-bonding interactions of the compound shown in **Fig.3** and the values are given in **Table 2**.

**Fig.3.** H-Bonding interaction of the molecule

3.4. HOMO-LUMO analysis

Frontier molecular orbitals such as highest occupied molecular orbital (HOMO) and lowest unoccupied molecular orbital (LUMO) are the most important in quantum mechanics. These orbitals play a vital role in analyzing the electrical optical properties of the molecule and also the interaction of various charge transfer systems. The highest occupied molecular orbital which carries electron with high energy and can ability to donate electron which is recognized as an electron donor (nucleophile character). Conversely, the lowest unoccupied molecular orbital (LUMO) with the least energy tends to accept electron density which is recognized as an electron acceptor (electrophilic character) [38]. These orbitals

are the most important for describing the perspective site in the π electronic system.

Table 2. H- Bonding interaction (Symmetry codes: (i) 1-x,1-y,-z)

D-H...A	D-H	H...A	D...A	D-H...A
N1-H1A...O1 ⁽ⁱ⁾	0.84(2)	2.14(2)	2.9821(17)	173.1(19)
C4-H4...O3	1.01(2)	2.51(2)	3.133(2)	119.5(16)
C5-H5...O4 ⁽ⁱ⁾	0.96(2)	2.47(2)	3.377(2)	158.1(17)
C7-H7...O1	0.986(15)	2.432(17)	2.8158(18)	102.6(11)
C7-H7...O3	0.986(15)	2.351(17)	2.7291(18)	101.8(11)
C18-H18A...O2	0.96	2.38	2.7688(19)	104

The molecular reactivity, kinetic stability, and polarisability of the molecule were described via the energy gap between HOMO-LUMO. The softness and hardness of the molecule were determined by the energy gap [39]. If the energy gap between HOMO-LUMO is high, the molecule possesses hardness, lesser polarisability, low chemical reactivity, and greater kinetic susceptibility. On the contrary, the lower energy gap between HOMO-LUMO leads to the softness of the molecule with greater polarisability, high chemical reactivity and lower kinetic stability. The potential of charge-transfer interactions of the molecule is also explained by the energy gap [40].

The electronic transitions of the compound were studied through HOMO-LUMO analysis using Gaussian 09 software. The intramolecular charge movement between electron donor and electron acceptor is (HOMO-LUMO) shown in **Fig. 4**. The geometric parameters of the crystal phase and DFT phase are given in **Table S3**. The calculated $E_{\text{HOMO}} = -5.83\text{eV}$, $E_{\text{LUMO}} = -1.32\text{eV}$ and the energy gap between them $E_{\text{gap}} = 4.34\text{eV}$, this value indicates that the molecule has high chemical reactivity and low kinetic stability.

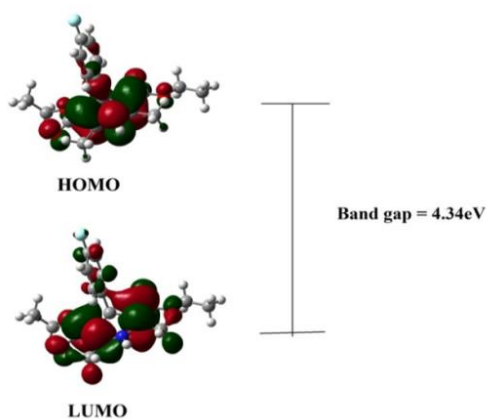


Fig. 4. 3-Dimensional HOMO-LUMO surface

The DFT mapped surface shown in **Fig. 4** indicate that HOMO is localized over the benzene and pyridine ring of the compound, excluding methyl and ethyl groups, whereas the LUMO has spread over pyridine and aromatic ring. The energy gap of the crystal phase is found to be $E_{\text{gap}} = 4.53\text{eV}$ which has a good correlation with $E_{\text{gap}} = 4.34\text{eV}$ calculated by DFT method. The energy gap and molecular descriptors are given in **Table 3**.

Table 3. Molecular descriptors of Crystal phase and DFT phase

Molecular descriptors	Crystal phase Energy (eV)	DFT phase
Electron affinity $A = [-E_{\text{LUMO}}]$	1.329549	1.523022
Ionization potential $I = [-E_{\text{HOMO}}]$	5.83358	5.865961
Global hardness $\eta = (I+A)/2$	2.252015	2.17147
Electrochemical potential $\mu = -(I+A)/2$	-3.58156	-3.69449
Electrophilicity $\omega = \mu^2/2\eta$	1.099462	1.16343
Electronegativity $\chi = (I+A)/2$	3.581564	3.694492
HOMO energy	-5.833579	-5.865961
LUMO energy	-1.329549	-1.5230221

3.5. Molecular Electrostatic potential analysis (MEP)

The hydrogen binding interaction of the molecule depends on electrophilic and nucleophilic effects which are determined by molecular electrostatic potential (MEP). The DFT solved geometries were

plotted against electrophilic and nucleophilic characters. The 3D ESP surface of the compound was visualized by different colors, in which electron-rich site appears at the red color, (most negative) and electron deficient-site appears at blue color (most positive). The yellow and light blue color indicates slightly electron deficient site [41,42]. MEP surface of the compound shown in **Fig. 5** reveals that the electron density is found to be more on the oxygen atom of the carbonyl group possesses negative charge results in electrophilic character. The blue color appears at NH- of the pyridine ring which is favorable for nucleophilic character. The yellow and light blue color appears on the alkyl and benzene ring which indicate slightly electron deficient region.

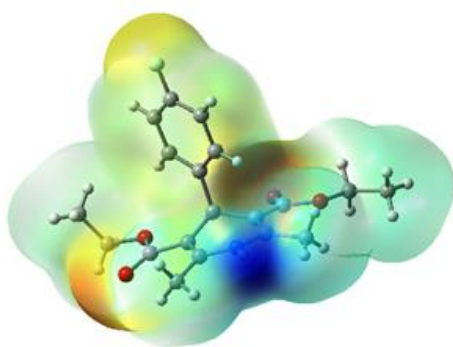


Fig 5. MEP plot of the molecule

3.6. MPA and NPA analysis

The charge distribution of the molecule was evaluated by Mulliken population analysis (MPA) and Natural population analysis (NPA) by DFT method [43,44]. The calculated MPA and NPA values of the compound (DFT phase and Crystal phase) are given in **Table S4**. The carbon atoms (C6, C9, C10, C12 and C15) of the compound were observed at +Ve region and (C1, C2, C3, C4, C5, C7, C8, C11, C13, C14, C16, C17, C18 and C19) were observed in - Ve region. The pyridine ring contains nitrogen atom and oxygen atoms of the ethoxy group (O1, O2, O3, and O4) were observed in -Ve region. The F atom of the compound (phenyl ring) was observed in -Ve region and all the H atoms were found only in +Ve region.

3.7. Antimicrobial analysis

Antimicrobial study of the compound was determined by well diffusion method against the microorganisms such as *Bacillus subtilis*,

Staphylococcus aureus, *Escherchia coli*, *Pseudomonas aeruginosa*, *Candida albicans* and *Aspergillus niger* at Eumic analytical Lab and Research Institute, Tiruchirappalli. The microorganisms and maintained by periodically sub cultured by Nutrient agar and Sabouraud dextrose medium for bacteria and fungi respectively. The plates inoculated by the bacteria and fungi were incubated for 24 h (37°C) 72 h (27°C) for fungi respectively. The inhibition zone of microbial growth surrounded by filter paper disc (5mm) was measured in millimeters. The effect produced by the sample was compared with the positive control (standard amoxicillin 100 µL/disc for bacteria; Nystatin 100 µL/disc for fungi) and the solvent-DMSO. The results of in-vitro antimicrobial activity of the compound indicate that better inhibition against *Bacillus subtilis* and *Escherchia coli* at 100µL. The antimicrobial zone of inhibition shown in **Fig. 6** and inhibition activity of the compound is shown in **Fig.7**.

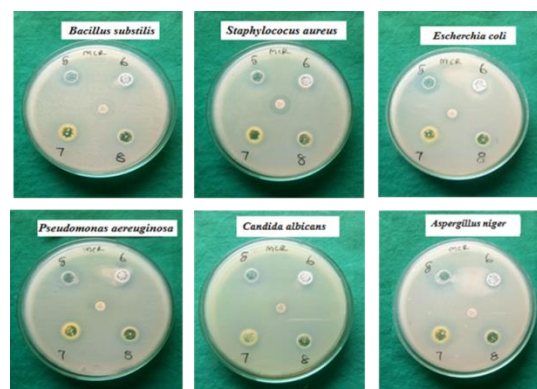


Fig. 6. Zone of inhibition

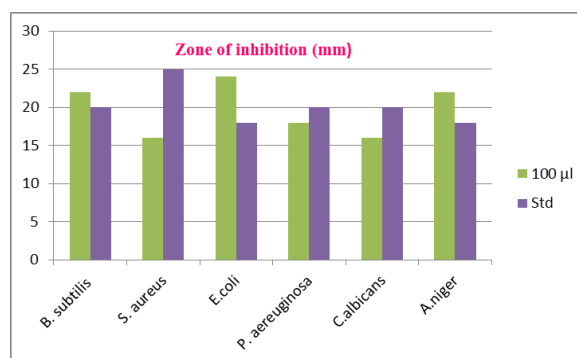


Fig. 7. Inhibition activity

4. Conclusion

The title compound was synthesized and crystal structure was established through SC-XRD analysis and it belongs to the monoclinic crystal system and Goodness of fit on F2 =1.057. The crystallographic parameters are in good agreement with DFT calculation. The HOMO-LUMO analysis of the compound shows the molecular charge-transfer is 4.34eV (energy gap), which indicates that the compound is more reactive and more stable. The molecular orbital energies of the crystal and DFT are found to be (HOMO = -5.83eV and -5.86eV) and (LUMO = -1.32eV and -1.52eV) respectively. The GCRD parameters revealed that the compounds possess negative value of chemical potential (-3.58 eV) and lesser value of electrophilicity index (1.09eV) which are indicates the stability and nucleophilic character respectively. The molecular electrostatic potential studies revealed that alkyl and benzene ring are in the most positive region which is more favorable for the nucleophilic character. The in-vitro antimicrobial activity results indicate that the compound shows better inhibition activity against *Bacillus subtilis*, *Escherchia coli* and *Aspergillus niger* at 100µL.

5. Acknowledgments

We record our sincere thanks to the Centre for Instrumentation and Maintenance Facility (CIMF), Periyar University, Salem for providing the facilities for single crystal XRD analysis and SAIF-VIT for providing ¹H, ¹³C NMR analysis. The author's also place their gratitude to Jamal instrumentation facility (JIF), Post Graduate and Research Department of Chemistry, Jamal Mohamed College, Tiruchirappalli for providing necessary lab facilities.

References

- [1] Hantzsch, A. 1881, EurJIC, Condensationsprodukte aus Aldehydammoniak undketonartigen Verbindungen
- [2] L. Xu, D.Li, L.Tao, Y.Yang, Y.Li, T.Hou, *Mol. Biosyst.* 12 (2016), 379–390.
- [3] A.Velena, N. Zarkovic, K. Gall Troselj, E. Bisenieks, J. Krauze, A.Poikans, G. Duburs, *Oxid. Med. Cell. Longev.* (2016), 1–35.
- [4] J. Yang, C. Jiang, J.Yang, C.Qian, D.Fang, *Green Chem. Lett. Rev.* 6 (2013) 262–267.
- [5] J. Kuthan, A. Kurfur'st *Ind Eng Chem Prod Res Dev* (1982) 21-191
- [6] R. J. Chorvat, K.J. Roring, *J. Org. Chem.* 53 (1988) 5779
- [7] A. Guzman, M. Romero, A. Maddox, J. Muchowski, *J Org Chem* 55(1990), 5793
- [8] C.O. Kappe, *Tetrahedron* 49(1993), 6937
- [9] B.Love, M. Goodman, K.M Snader, R.Tedeschi, E. Macko, *J. Med. Chem.* 17 (1974), 956–965.
- [10] P.K. Gilpin, L.A. Pachla, *Anal. Chem.* 71 (1999), 217–233.
- [11] S. Cosconati, L.Marinelli, A. Lavecchia, E. Novellino, *J. Med. Chem.* 50 (2007), 1504–
- [12] F.Bossert, W.Vater, *Med Res Rev.* 9 (1989), 531
- [13] D.J. Triggle, *Mini-Rev Med Chem* 3(2003), 215
- [14] Triggle, D.J. *Cell Mol Neurobiol.* 23(2003), 293
- [15] K.M.M. Murphy, R.J. Gould, B.L.Largent, S.H. Synder, *Proc Natl Acad Sci USA* 80 (1983), 860
- [16] S. Goldmann, J.Stolefuss, *Angew Chem Int De Engl* 30 (1991), 1559
- [17] M. Schramm, G. Thomas, R. Towart, G. Franckowiak, *Nature* 303 (1983), 535
- [18] R. Budriesi, A.Bisi, P. Ioan, A.Rampa, S. Gobbi, F. Bulleti, L.Piazzzi, P. Valenti, A. Chiarini, *Bioorg Med Chem* 13(2005), 3423
- [19] S. Naveen, S.J. Prasad, D. Manvar, A. Mishra, A. Shah, *J Chem Crystallogr* 38 (2008) 315
- [20] D.R. Ferry, H. Glossmann, Naunyn Schmiedeberg's, *Arch Pharmacol* 321 (1982), 80
- [21] T.M. Itil, S.T. Michael, F. Hoffmeister, A. Kunitz, E. Eralp, *Curr Ther Res* 35(1984), 405
- [22] F. Lentz, N.Reiling, G.Spengler, A. Kincses, A. Csonka, J. Molnár, A. Hilgeroth, *Molecules.* 24 (2019)2873.
- [23] A.M. Vijesh, A.M. Isloor, S.K. Peethambar, K.N. Shivananda, T. Arulmoli, N.A.Isloor, *E. J. Med. Chem.* 46 (2011) 5591–5597.
- [24] M. Kataria, S. Pramanik, M. Kumar, V. Bhalla, *Chem. Com.* 51 (2015), 1483–1486.
- [25] L. Shen, S. Cao, J. Wu, J.Zhang, H.Li, N.Liu, X. Qian, *Green Chem.* 11 (2009), 1414–1420.
- [26] H.M. Patel, K.D. Patel, H.D. Patel, *Curr. Bioact. Compd.* 13 (2017), 47–58.
- [27] Bruker, APEX2, SAINT, and SADABS, (2006).
- [28] G.M. Sheldrick, SADABS Bruker Axs Inc, Madison, Wisconsin, USA, 2007.

- [29] G.M. Sheldrick, *Acta Crystallogr. Sect. A Found. Crystallogr.* 64 (2008) 112–122,
- [30] G.M. Sheldrick, *Acta Crystallogr. Sect. C Struct. Chem.* 71 (2015) 3–8.
- [31] C.F. Macrae, P.R. Edgington, P. McCabe, E. Pidcock, G.P. Shields, R. Taylor, M. Towler, J. Van De Streek, *J. Appl. Crystallogr.* 39 (2006) 453–457.
- [32] L.J. Farrugia, *J. Appl. Cryst.* 45 (2012) 849 – 854.
- [33] A.D. Becke, *Phys. Rev. A.* 38 (1998), 3098.
- [34] D. Hayakawa, N. Sawada, Y. Watanabe, H. Gouda, *J. Mol. Graph. Model.* 96 (2020), 107515.
- [35] M. G. Sharma, D. P. Rajani, H. M. Patel, *R. Soc. open sci.* 4 (2017) 170006.
- [36] Leila Moradi, Roya Mahinpour, Zohreh Zahraei, Nafiseh Pahlevanzadeh, *Journal of Saudi Chem. Society.* 7 (2018) 876-885.
- [37] Srinivas Nayak Amgoth, Mahendar Porika Sadanandam Abbagani, Achaiah Garlapati, Malla Reddy Vanga, *Med Chem Res.* 22 (2013)147–155.
- [38] R. Ricardo Ternavisk, J. Ademir Camargo, B. C. Francisco Machado, A. Jose F. F. Rocco, L. Gilberto B. Aquino, Valter H. C. Silva, Hamilton B. Napolitano, *J. Mol. Structure* 20 (2014) 2526.
- [39] Raja, M. Raj Muhamed, R. Muthu, S. Suresh, *M. J. Mol. Struct.* 1141, 5 (2017) 284-298,
- [40] R. Kumar, A. Kumar, V. Deval, A. Gupta, P. Tandon, P. S. Patil, P. Deshmukh, D. Chaturvedi, J.G. Watve, *J. Mol. Struct.* 1129 (2017) 292-304.
- [41] A.Dhandapani, M. Suresh, *J. Mol. Struct.* (2020)129484.
- [42] Hena Khanum, Ashraf Mashrai, Nazish Siddiqui, Musheer Ahmad, Mohammad Jane Alam, Shabbir Ahmad, Shamsuzzaman, *J. Mol. Struct.* 1084 (2015) 274-283.
- [43] J.C. Dobson, A. Hinchliffe, Mulliken *J. Mol. Struct.* 27 (1975) 161-166. Z. Demircioğlu, C.A. Kaştaş, O. Büyükgüngör, *J. Mol. Struct.* 1091 (2015) 183-195.
- [44] Z. Demircioğlu, C.A. Kaştaş, O. Büyükgüngör, *J. Mol. Struct.* 1091 (2015) 183-195.